

Quadrupolar and hexapolar Hall magnetic field during asymmetric magnetic reconnection without a guide field

Longlong Sang, Quanming Lu, Rongsheng Wang, Kai Huang, and Shui Wang

Citation: [Physics of Plasmas](#) **25**, 062120 (2018); doi: 10.1063/1.5030439

View online: <https://doi.org/10.1063/1.5030439>

View Table of Contents: <http://aip.scitation.org/toc/php/25/6>

Published by the [American Institute of Physics](#)

PHYSICS TODAY

WHITEPAPERS

MANAGER'S GUIDE

Accelerate R&D with
Multiphysics Simulation

READ NOW

PRESENTED BY

 **COMSOL**

Quadrupolar and hexapolar Hall magnetic field during asymmetric magnetic reconnection without a guide field

Longlong Sang, Quanming Lu,^{a)} Rongsheng Wang,^{a)} Kai Huang, and Shui Wang
 CAS Key Laboratory of Geospace Environment, School of Earth and Space Sciences,
 University of Science and Technology of China, Hefei 230026, China

(Received 21 March 2018; accepted 2 June 2018; published online 20 June 2018)

In this paper, by taking advantage of a two-dimensional particle-in-cell simulation model, we study the structure of the out-of-plane magnetic field (Hall magnetic field) during asymmetric magnetic reconnection without a guide field, and the associated in-plane current system is also analyzed. The evolution of asymmetric reconnection has two stages. At the first stage, the electrons move toward the X line along the separatrix in the magnetosheath side, and depart from the X line along the separatrix in the magnetosphere side. Another electron flow toward the X line exists above the separatrix in the magnetosphere side. The resulted in-plane current system, which is mainly determined by electron dynamics, generates the quadrupolar structure of the Hall magnetic field, where the two quadrants in the magnetosheath side are much stronger than those in the magnetosphere side. At the second stage, besides these electron flows, an additional electron flow away from the X line is formed along the magnetic field below the separatrix in the magnetosheath side. A hexapolar structure of the Hall magnetic field is then generated by such a current system. *Published by AIP Publishing.*

<https://doi.org/10.1063/1.5030439>

I. INTRODUCTION

As a fundamental physical plasma process, magnetic reconnection plays an important role to convert rapidly magnetic energy into plasma kinetic and thermal energy.^{1–3} In the earth's magnetosphere, magnetic reconnection may occur in both the dayside magnetopause and magnetotail,^{4–12} where the classical collision between charged particles is negligible and the plasma is collisionless. The diffusion region in collisionless magnetic reconnection is found to have a multi-scale structure: in the ion diffusion region with the scale size below c/ω_{pi} (where c/ω_{pi} is the ion inertial length), ions are demagnetized, while electrons are magnetized and frozen in the magnetic field; therefore, the motions between ions and electrons are different;^{5–7,13–20} in the electron diffusion region with the scale size below c/ω_{pe} (where c/ω_{pe} is the electron inertial length), even electrons are unmagnetized. Years of researches have shown a pretty beautiful and clear picture of symmetric magnetic reconnection, in which the plasma parameters (such as density, temperature, and the strength of magnetic field) are similar in both sides of the current sheet. Numerous kinetic simulations as well as Hall and electron magnetohydrodynamics (MHD) theories/simulations of symmetric magnetic reconnection have predicted that the Hall effect resulted from the decoupled motions between ions and electrons in the ion diffusion region leads to the in-plane current and then produces the quadrupolar structure of the out-of-plane magnetic field (Hall magnetic field).^{14–18,20,21} Satellite observations of magnetic reconnection in the earth's magnetotail, where the current sheet is considered to be symmetric, have also identified the quadrupolar configuration of the out-of-plane magnetic field. The quadrupolar structure of

the out-of-plane magnetic reconnection is now regarded as one of critical signatures of collisionless magnetic reconnection in a symmetric current sheet, although the introduction of guide field will distort the symmetry of the quadrupolar structure.^{22–27}

In asymmetric magnetic reconnection, where the plasma parameters are different in two sides of the current sheet, which kind of structure the out-of-plane magnetic field will be formed is still under debate. The dayside magnetopause, where the plasma parameters are different between the magnetosheath and magnetosphere, provides a suitable place to study asymmetric magnetic reconnection. Typically, in the magnetosheath side, the plasma density is about $0.3\text{--}0.5\text{ cm}^{-3}$ and the strength of magnetic field can be up to 50 nT, while in the magnetosphere side, the plasma density is about 20 cm^{-3} , and the magnetic field is 10–20 nT. Mozer *et al.*²⁸ observed a bipolar Hall magnetic field in a magnetopause reconnection event with THEMIS spacecraft. Recently, with the launching of MMS spacecraft, the structure of the Hall magnetic field in dayside magnetopause reconnection has been extensively studied. Although the spatial size and amplitude of the two quadrants in the magnetosheath side is much larger than those in the magnetosphere side, a quadrupolar configuration of the Hall magnetic field can still be clearly identified.^{11,29,30} Kinetic simulations of asymmetric reconnection also presented controversial results on the structure of the Hall magnetic field. Several predicted the quadrupolar pattern of the Hall magnetic field,^{31–33} while others showed the bipolar structure which exists only in the magnetosheath side.^{26,34–36} In this paper, we also perform two-dimensional (2-D) particle-in-cell (PIC) simulations of asymmetric reconnection without a guide field and investigate the evolution of the Hall magnetic field. We find that at first the Hall magnetic field forms a quadrupolar structure, and it evolves into a hexapolar

^{a)}Authors to whom correspondence should be addressed: qmlu@ustc.edu.cn and rswan@ustc.edu.cn

structure. The in-plane current system (Hall current system) has also been analyzed in this paper to understand the formation of such a structure of the Hall magnetic field.

II. SIMULATION MODEL

In this paper, we take advantage of a 2-D PIC simulation model to analyze the in-plane current and configuration of the Hall magnetic field in asymmetric magnetic reconnection without a guide field. In the model, the electric and magnetic fields are defined on the grids in a two-dimensional plane (the $x - z$ plane) and updated by solving Maxwell equations with an explicit algorithm. The current and charge densities appearing in Maxwell equations are accumulated on the grids from the particle data. The particles (both ions and electrons) move in a two-dimensional plane (the $x - z$ plane) under the action of the Lorentz force, and their three velocity components are all retained. The particle motions can be known by integrating the New-Lorentz equations with a leapfrog scheme. The model has been successfully used to study collisionless magnetic reconnection and plasma waves in the magnetosphere.^{18,37,38} Initially, the magnetic field is expressed by $\mathbf{B}(z) = B_0[\tanh(z/\lambda) + 1/2]\mathbf{e}_x$ (where λ is the half width of the current sheet), and the number density is $n = n_0[1 - (1/3)\tanh(z/\lambda) - (1/3)\tanh^2(z/\lambda)]$. The magnetic field changes from $3B_0/2$ in the magnetosphere side to $-B_0/2$ in the magnetosheath side, and the number density varies from $n_0/3$ in the magnetosphere side to n_0 in the magnetosheath side. Both electrons and ions are assumed to have the Maxwellian velocity distribution with a uniform temperature. We choose the initial electron to ion temperature ratio as $T_{e0}/T_{i0} = 1/3$ (where the subscripts e and i represent electron and ion, respectively). The light speed is $c = 20V_{A0}$ (where V_{A0} is the Alfvén speed, which is calculated with B_0 and n_0). The mass ratio of ion to electron is $m_i/m_e = 100$. The width of the current sheet is $\lambda = 0.5 d_i$ (where $d_i = c/\omega_{pi}$, and ω_{pi} is the ion plasma frequency calculated with n_0). The details of the initial setup can be found in Ref. 26.

The simulation domain is $L_x \times L_z = 54d_i \times 22.5d_i$, and the grid number is 1080×450 . Therefore, the grid size is $\Delta x = \Delta z = 0.05c/\omega_{pi}$. The time step is $\Delta t = 0.001\Omega_i^{-1}$ (where Ω_i is the ion gyrofrequency, which is calculated with B_0). Each species has at least 6×10^8 particles. In the z direction, conducting boundary conditions are used for the electromagnetic fields and particles are reflected in the boundary, while periodic boundary conditions are employed in the x direction for both electromagnetic fields and particles. To make a quick reconnection onset, a small perturbation to the magnetic flux function is assumed initially with the formula $\Delta\psi = \psi_0 \cosh^{-2}(2z/\lambda) \cosh^{-2}(x/2)$, and $\psi_0 = 0.05cB_0/\omega_{pi}$.

III. SIMULATION RESULTS

The time evolution of asymmetric magnetic reconnection can be followed in Fig. 1, which plots the configuration of the Hall magnetic field B_y/B_0 at $\Omega_i t = 10, 37$, and 50 . The magnetic field lines from the magnetosphere and magnetosheath begin to reconnect at about $\Omega_i t = 10$, and the X line is formed around $(x, z) = (0, -0.3d_i)$, which is in the magnetosheath side. The Hall magnetic field B_y begins to form a

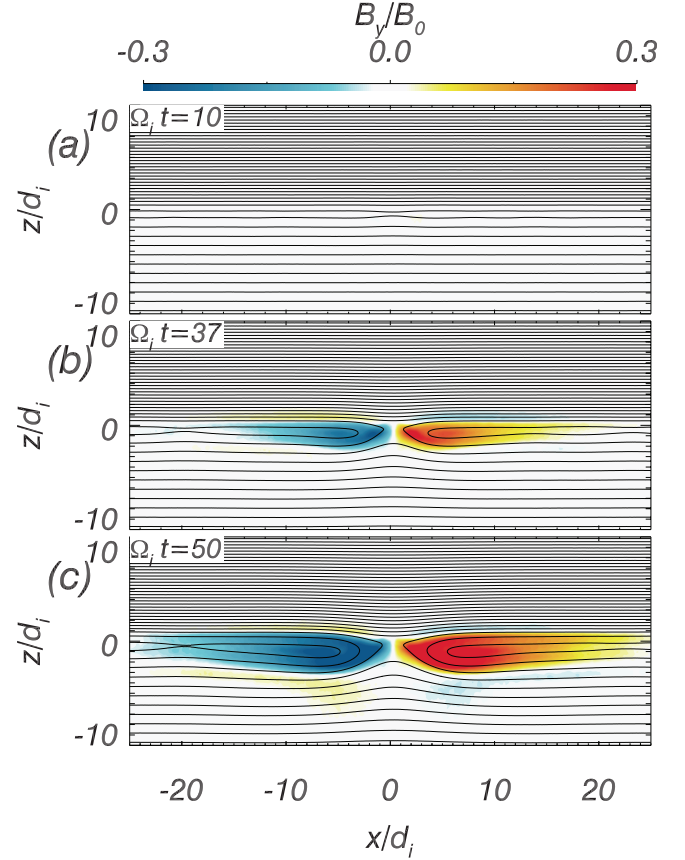


FIG. 1. The time evolution of the Hall magnetic field B_y in asymmetric reconnection at (a) $\Omega_i t = 10$, (b) $\Omega_i t = 37$ and (c) $\Omega_i t = 50$, respectively. The black lines plot the magnetic field lines in the reconnection plane.

quadrupolar structure at about $\Omega_i t = 30$, and it becomes salient at $\Omega_i t = 37$. The quadrupolar Hall magnetic field is dominated by the two quadrants in the magnetosheath side. The width of the quadrants in the magnetosheath is about $2.0d_i$, and the amplitude is about $0.3B_0$. In the magnetosphere side, the width of the quadrants in the magnetosphere is about $0.9d_i$, and the amplitude is about $0.04B_0$. The quadrupolar structure of the Hall magnetic field has been previously identified in asymmetric reconnection with both kinetic simulations^{31–33} and MMS observations.^{11,29,30} However, from about $\Omega_i t = 45$, below the quadrupolar structure, another Hall magnetic field B_y , whose width and amplitude are, respectively, about $1.0d_i$ and $0.04B_0$, begins to be generated in the magnetosheath side, and its polarity is opposite to that of the dominated quadrants. Then, a hexapolar structure of the out-of-plane magnetic field is formed, which can be seen clearly at $\Omega_i t = 50$.

The Hall magnetic field B_y is generated by the in-plane current system. Figure 2 plots (a) the in-plane current in the parallel direction $J_{\parallel} = \mathbf{J} \cdot \mathbf{B}'/B'$ (where $\mathbf{B}' = B_x\mathbf{e}_x + B_z\mathbf{e}_z$ and $\mathbf{J}' = J_x\mathbf{e}_x + J_z\mathbf{e}_z$ are the in-plane magnetic field and current), (b) the in-plane current in the perpendicular direction $J_{\perp} = |\mathbf{J}' - J_{\parallel}\mathbf{B}'/B'|$, and (c) the cut of the in-plane current in the parallel direction (J_{\parallel}) along $x = -2.2d_i$ at $\Omega_i t = 37$. At this time, the Hall magnetic field has a salient quadrupolar pattern. Because the electrons are magnetized in the separatrix region and move along the magnetic field, the in-plane

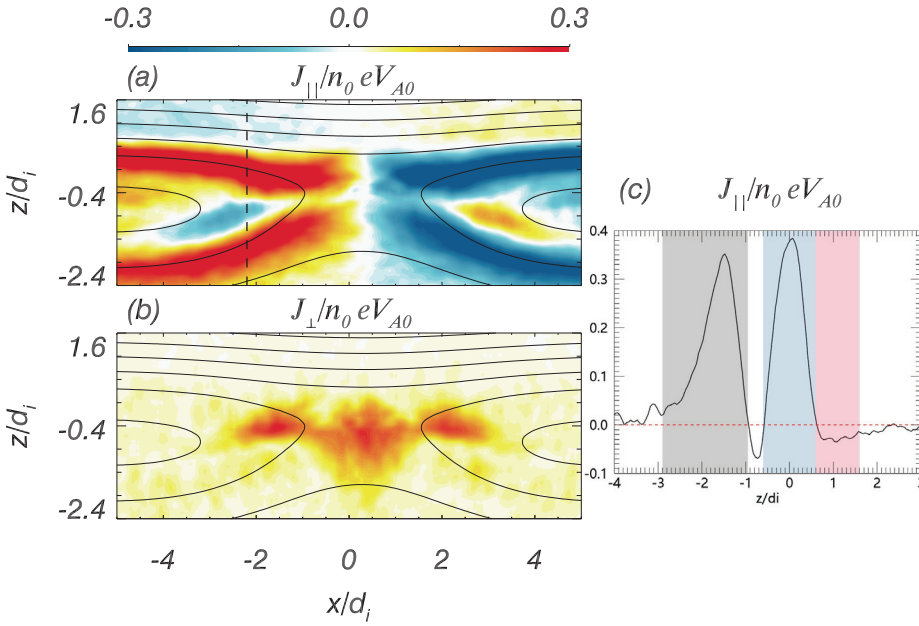


FIG. 2. The distributions of the in-plane current in (a) the parallel direction $J_{\parallel} = \mathbf{J}' \cdot \mathbf{B}'/B'$ (where $\mathbf{B}' = B_x \mathbf{e}_x + B_z \mathbf{e}_z$ and $\mathbf{J}' = J_x \mathbf{e}_x + J_z \mathbf{e}_z$ is the in-plane magnetic field and current), and (b) the perpendicular direction $J_{\perp} = |\mathbf{J}' - J_{\parallel} \mathbf{B}'/B'|$ at $\Omega_i t = 37$. (c) The cut of the in-plane current in the parallel direction J_{\parallel} along $x = -2.2 d_i$ at $\Omega_i t = 37$.

current in the parallel direction is concentrated in the separatrix region. In the vicinity of the X line, electrons are unfrozen in the magnetic field, and the in-plane current in the perpendicular direction is then generated. The in-plane current in the parallel direction is much larger than that in the perpendicular direction around the separatrix region. Previous kinetic simulations of asymmetric magnetic reconnection have shown that the in-plane current points toward the X line along the separatrix in the magnetosphere side and flows away along the separatrix in the magnetosheath side,²⁶ and such a kind of in-plane current system creates the enhancement of B_y with a bipolar pattern in the outflow region. However, in our simulations, there still exists another small in-plane current above the separatrix in the magnetosphere side, which can be seen clearly in Fig. 2(c). The gray area represents the current away from the X line in the magnetosheath side, and the light blue area shows the current toward the X line in the magnetosphere side. The pink area is another current which leaves away from the X line in the magnetosphere side. Such an in-plane current system generates a distorted quadrupolar structure of Hall magnetic field shown in Fig. 1(b), where the quadrants in the magnetosheath side are much stronger than that in the magnetosphere side.

Figure 3 presents (a) the parallel component of the electron bulk velocity $V_{e\parallel} = \mathbf{V}_e \cdot \mathbf{B}'/B'$ (where $\mathbf{B}' = B_x \mathbf{e}_x + B_z \mathbf{e}_z$ is the in-plane magnetic field), and (b) the parallel component of the ion bulk velocity $V_{i\parallel} = \mathbf{V}_i \cdot \mathbf{B}'/B'$ at $\Omega_i t = 37$. Obviously, the parallel component of the ion bulk velocity is much smaller than that of the electron bulk velocity, and the parallel component of the in-plane current existing around the separatrix region is mainly contributed by the electrons. The electrons flow toward the X line along the magnetosheath separatrix and leave away from the X line along the magnetosphere separatrix. Besides, above the separatrix in the magnetosphere side, the electrons tend to move toward the X line along the magnetic field with the speeds about $0.1 V_{A0}$. The electrons, which move toward the X line in both the

magnetosheath and magnetosphere sides, are subject to the parallel acceleration by the parallel electric field and the mirror force. After they are accelerated further by the reconnection electric field near the X line, the electrons leave away along the magnetosphere separatrix.^{20,39} These electron motions lead to the in-plane current system depicted in Fig. 2.

Figure 4 plots (a) the in-plane currents in the parallel direction, (b) the in-plane current in the perpendicular direction $J_{\perp} = |\mathbf{J}' - J_{\parallel} \mathbf{B}'/B'|$, and (c) the cut of the in-plane current in the parallel direction (J_{\parallel}) along $x = -15 d_i$ at $\Omega_i t = 50$. At this time, the Hall magnetic field has a hexapolar pattern. Similarly, the in-plane currents in the parallel and perpendicular directions are concentrated in the separatrix region and the vicinity of the X line, respectively. Now, in

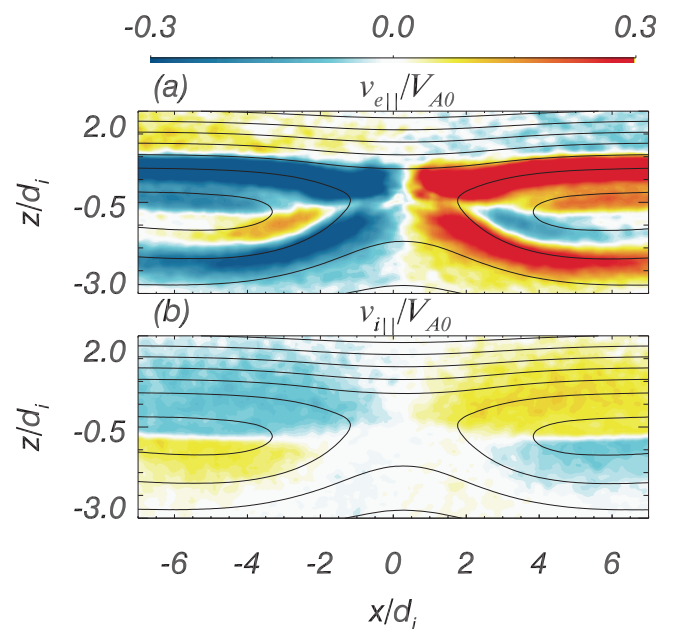


FIG. 3. The parallel component of electron bulk velocity $V_{e\parallel} = \mathbf{V}_e \cdot \mathbf{B}'/B'$ (where $\mathbf{B}' = B_x \mathbf{e}_x + B_z \mathbf{e}_z$ is the in-plane magnetic field), and (b) the parallel component of ion bulk velocity $V_{i\parallel} = \mathbf{V}_i \cdot \mathbf{B}'/B'$ at $\Omega_i t = 37$.

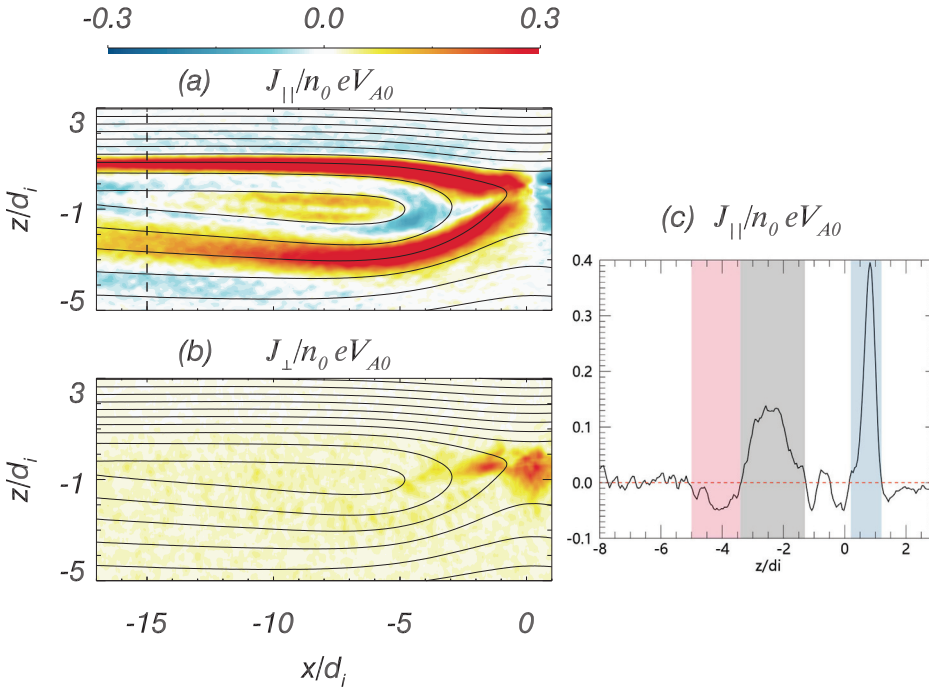


FIG. 4. The distributions of the in-plane current in (a) the parallel direction $J_{\parallel} = \mathbf{J}' \cdot \mathbf{B}'/B'$ (where $\mathbf{B}' = B_x \mathbf{e}_x + B_z \mathbf{e}_z$ and $\mathbf{J}' = J_x \mathbf{e}_x + J_z \mathbf{e}_z$ is the in-plane magnetic field and current), and (b) the perpendicular direction $J_{\perp} = |\mathbf{J}' - J_{\parallel} \mathbf{B}'/B'|$ at $\Omega_i t = 37$. (c) The cut of the in-plane current in the parallel direction J_{\parallel} along $x = -15d_i$ at $\Omega_i t = 50$.

addition to the currents described in Fig. 2, there still exists another in-plane current along the magnetic field below the separatrix in the magnetosheath side, and the current points toward the X line. This current can be exhibited more clearly in Fig. 4(c), which is denoted by the pink area. The resulted in-plane current system generates the hexapolar pattern of the Hall magnetic field illustrated in Fig. 1(c). Figure 5

exhibits (a) the parallel component of the electron bulk velocity $V_{e\parallel} = \mathbf{V}_e \cdot \mathbf{B}'/B'$ and (b) the parallel component of the ion bulk velocity $V_{i\parallel} = \mathbf{V}_i \cdot \mathbf{B}'/B'$ at $\Omega_i t = 50$. The parallel component of the ion bulk velocity is much smaller than that of the electron bulk velocity, and the current is mainly carried by electrons. Corresponding to the in-plane current pointing the X line along the magnetic field below the separatrix in the magnetosheath side, the electrons leave away from the X line along the magnetic field. We can find an obvious pileup of magnetic field around $(x, z) = (-5.0d_i, -1.5d_i)$ in the magnetosheath side, which makes the electrons therein leave away the X line along the magnetic field due to the mirror force, and produces the parallel current pointing to the X line below the magnetosheath separatrix.²⁰

IV. SUMMARY AND DISCUSSION

In this paper, with a 2-D PIC simulation model, we investigate the generation of the structure of the Hall magnetic field in asymmetric magnetic reconnection without a guide field. In the simulation, we at first observe the quadrupolar Hall magnetic field, where both the strength and size of the generated out-of-plane magnetic field in the magnetosheath side are much stronger than those in the magnetosphere side. At this stage, the electrons flow toward the X line along the separatrix in the magnetosheath side and leave away from the X line along the separatrix in the magnetosphere side, while the third electron flow is moving toward the X line along the magnetic field above the separatrix in the magnetosphere side. The resulted current system produces the quadrupolar structure of the Hall magnetic field at this stage. At the second stage, there still exists an additional electron flow away from the X line along the magnetic field below the separatrix in the magnetosheath side, and the current system leads to the hexapolar structure of the Hall magnetic field.

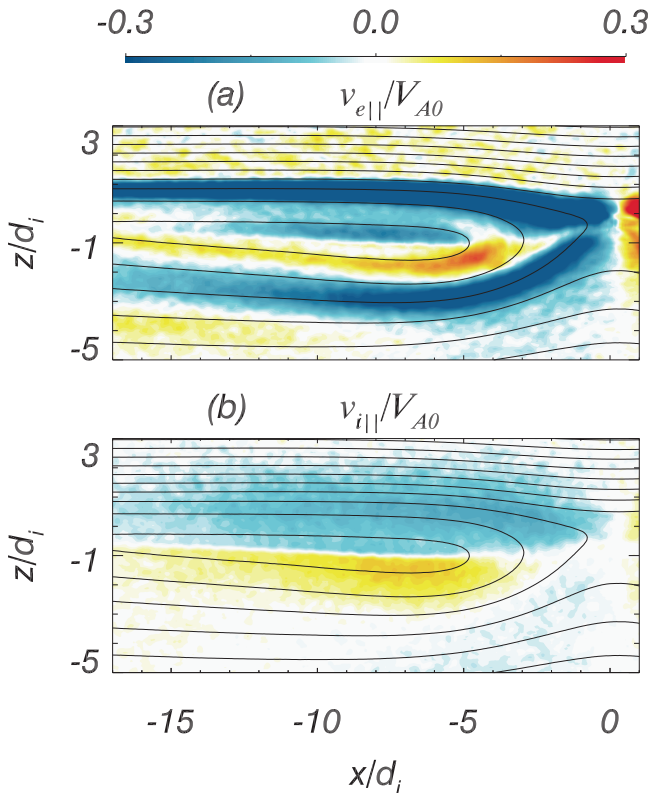


FIG. 5. The parallel component of electron bulk velocity $V_{e\parallel} = \mathbf{V}_e \cdot \mathbf{B}'/B'$ (where $\mathbf{B}' = B_x \mathbf{e}_x + B_z \mathbf{e}_z$ is the in-plane magnetic field), and (b) the parallel component of ion bulk velocity $V_{i\parallel} = \mathbf{V}_i \cdot \mathbf{B}'/B'$ at $\Omega_i t = 50$.

Magnetic reconnection events, which occur in the dayside of the earth's magnetopause, give a good opportunity to study asymmetric reconnection. However, satellite observations presented controversial results on the structure of the Hall magnetic field in asymmetric reconnection: the recent MMS spacecraft observed a quadrupolar structure,^{11,29,30} while the previous observations presented the bipolar structure.²⁸ Kinetic simulations also gave controversial conclusions on whether the Hall magnetic field has a bipolar or quadrupolar structure in asymmetric reconnection. Our simulations further predict that the Hall magnetic field in asymmetric reconnection may have a hexapolar structure. Therefore, the Hall magnetic field in asymmetric reconnection may have a complicated structure, and more simulations and observations at different plasma parameters are necessary to reveal it.

ACKNOWLEDGMENTS

This work was supported by the NSFC Grant Nos. 41527804, 41774169, 41474125, and 41331067, and the Key Research Program of Frontier Sciences, CAS (QYZDJ-SSW-DQC010).

- ¹V. M. Vasyliunas, *Rev. Geophys.* **13**, 303, <https://doi.org/10.1029/RG013i001p00303> (1975).
- ²D. Biskamp, *Magnetic Reconnection in Plasmas* (Cambridge University Press, Cambridge, UK, 2000), p. 3.
- ³E. Priest and T. Forbes, *Magnetic Reconnection: MHD Theory and Applications* (Cambridge University Press, Cambridge, UK, 2000), p. 6.
- ⁴D. N. Baker, T. I. Pulkkinen, V. Angelopoulos, W. Baumjohann, and R. L. McPherron, *J. Geophys. Res.* **101**, 12,975, <https://doi.org/10.1029/95JA03753> (1996).
- ⁵M. Øieroset, T. D. Phan, M. Fujimoto, R. P. Lin, and R. P. Lepping, *Nature* **412**, 414 (2001).
- ⁶X. H. Deng and H. Matsumoto, *Nature* **410**, 557 (2001).
- ⁷T. Nagai, I. Shinohara, M. Fujimoto, M. Hoshino, Y. Saito, S. Machida, and T. Mukai, *J. Geophys. Res.* **106**, 25929, <https://doi.org/10.1029/2001JA900038> (2001).
- ⁸A. Vaivads, Y. Khotyaintsev, M. Andre, A. Retino, S. C. Buchert, B. N. Rogers, P. Decreau, G. Paschmann, and T. D. Phan, *Phys. Rev. Lett.* **93**, 105001 (2004).
- ⁹V. Angelopoulos, J. P. McFadden, D. Larson, C. W. Carlson, S. B. Mende, H. Frey, T. Phan, D. G. Sibeck, K. Glassmeier, U. Auster, E. Donovan, I. R. Mann, I. J. Rae, C. T. Russell, A. Runov, X. Z. Zhou, and L. Kepko, *Science* **321**, 931 (2008).
- ¹⁰R. S. Wang, Q. M. Lu, A. M. Du, and S. Wang, *Phys. Rev. Lett.* **104**, 175003 (2010).
- ¹¹R. S. Wang, R. Nakamura, Q. Lu, W. Baumjohann, R. E. Ergun, J. L. Burch, M. Volwerk, A. Varsani, T. Nakamura, W. Gonzalez, B. Giles, D. Gershman, and S. Wang, *Phys. Rev. Lett.* **118**, 175101 (2017).
- ¹²J. L. Burch, R. B. Torbert, T. D. Phan, L.-J. Chen, T. E. Moore, R. E. Ergun, J. P. Eastwood, D. J. Gershman, P. A. Cassak, M. R. Argall, S. Wang, M. Hesse, C. J. Pollock, B. L. Giles, R. Nakamura, B. H. Mauk, S. A. Fuselier, C. T. Russell, R. J. Strangeway, J. F. Drake, M. A. Shay, Y. V. Khotyaintsev, P.-A. Lindqvist, G. Marklund, F. D. Wilder, D. T. Young, K. Torkar, J. Goldstein, J. C. Dorelli, L. A. Avano, M. Oka, D. N. Baker, A. N. Jaynes, K. A. Goodrich, I. J. Cohen, D. L. Turner, J. F. Fennell, J. B. Blake, J. Clemmons, M. Goldman, D. Newman, S. M. Petriner, K. J. Trattner, B. Lavraud, P. H. Reiff, W. Baumjohann, W. Magnes, M. Steller, W. Lewis, Y. Saito, V. Coffey, and M. Chandler, *Science* **352**, aaf2939 (2016).
- ¹³B. U. Ö. Sonnerup, "Magnetic field reconnection," in *Solar System Plasma Physics*, edited by L. J. Lanzerotti, C. F. Kennel, and E. N. Parker (North-Holland Publishing Co., Amsterdam, 1979), Vol. 3, p. 46.
- ¹⁴Z. W. Ma and A. Bhattacharjee, *Geophys. Res. Lett.* **25**, 3277, <https://doi.org/10.1029/98GL02432> (1998).
- ¹⁵M. A. Shay and J. F. Drake, *Geophys. Res. Lett.* **25**, 3759, <https://doi.org/10.1029/1998GL900036> (1998).
- ¹⁶J. Birn, J. F. Drake, M. A. Shay, B. N. Rogers, R. E. Denton, M. Hesse, M. Kuznetsova, Z. W. Ma, A. Bhattacharjee, A. Otto, and P. L. Pritchett, *J. Geophys. Res.* **106**, 3715, <https://doi.org/10.1029/1999JA900449> (2001).
- ¹⁷W. Daughton, J. Scudder, and H. Karimabadi, *Phys. Plasmas* **13**, 072101 (2006).
- ¹⁸X. R. Fu, Q. M. Lu, and S. Wang, *Phys. Plasmas* **13**, 012309 (2006).
- ¹⁹R. S. Wang, Q. M. Lu, C. Huang, and S. Wang, *J. Geophys. Res.* **115**, A01209, <https://doi.org/10.1029/2009JA014553> (2010).
- ²⁰Q. M. Lu, C. Huang, J. L. Xie, R. S. Wang, M. Y. Wu, A. Vaivads, and S. Wang, *J. Geophys. Res.* **115**, A11208, <https://doi.org/10.1029/2010JA015713> (2010).
- ²¹S. V. Bulanov, F. Pegoraro, and A. S. Sakharov, *Phys. Fluids* **4**, 2499 (1992).
- ²²P. L. Pritchett and F. V. Coroniti, *J. Geophys. Res.* **109**, A01220, <https://doi.org/10.1029/2003JA009999> (2004).
- ²³J. P. Eastwood, M. A. Shay, T. D. Phan, and M. Øieroset, *Phys. Rev. Lett.* **104**, 205001 (2010).
- ²⁴S. Lu, Q. M. Lu, Y. Cao, C. Huang, J. L. Xie, and S. Wang, *Chin. Sci. Bull.* **56**, 48 (2011).
- ²⁵C. Huang, Q. M. Lu, and S. Wang, *Phys. Plasmas* **17**, 072306 (2010).
- ²⁶C. Huang, Q. M. Lu, S. Lu, P. R. Wang, and S. Wang, *J. Geophys. Res.* **119**, 798, <https://doi.org/10.1002/2013JA019249> (2014).
- ²⁷R. S. Wang, R. Nakamura, Q. Lu, A. Du, T. Zhang, W. Baumjohann, Y. V. Khotyaintsev, M. Volwerk, M. André, M. Fujimoto, T. K. M. Nakamura, A. N. Fazakerley, J. Du, W. Teh, E. V. Panov, B. Zieger, Y. Pan, and S. Lu, *J. Geophys. Res.* **117**, A07223, <https://doi.org/10.1029/2011JA017384> (2012).
- ²⁸F. S. Mozer, V. Angelopoulos, J. Bonnell, K. H. Glassmeier, and J. P. McFadden, *Geophys. Res. Lett.* **35**, L17S04, <https://doi.org/10.1029/2007GL033033> (2008).
- ²⁹F. Z. Peng, H. S. Fu, J. B. Cao, D. B. Graham, Z. Z. Chen, D. Cao, Y. Xu, S. Y. Huang, T. Y. Wang, Y. V. Khotyaintsev, M. Andre, C. T. Russell, B. Giles, P.-A. Lindqvist, R. B. Torbert, R. E. Ergun, and J. L. Burch, *J. Geophys. Res. Space Phys.* **122**, 6349, <https://doi.org/10.1002/2016JA023666> (2017).
- ³⁰Y. C. Zhang, B. Lavraud, L. Dai, C. Wang, A. Marchaudon, L. Avano, J. Burch, M. Chandler, J. Dorelli, S. P. Duan, R. E. Ergun, D. J. Gershman, B. Giles, Y. V. Khotyaintsev, P. A. Lindqvist, W. Paterson, C. T. Russell, C. Schiff, B. B. Tang, and R. Torbert, *J. Geophys. Res.* **122**, 5277, <https://doi.org/10.1002/2016JA023620> (2017).
- ³¹M. Swisdak, B. N. Rogers, J. F. Drake, and M. A. Shay, *J. Geophys. Res.* **108**(A5), 1218, <https://doi.org/10.1029/2002JA009726> (2003).
- ³²M. Hesse, N. Aunai, D. Sibeck, and J. Birn, *Geophys. Res. Lett.* **41**, 8673, <https://doi.org/10.1002/2014GL061586> (2014).
- ³³M. A. Shay, T. D. Phan, C. C. Haggerty, M. Fujimoto, J. F. Drake, K. Malakit, P. A. Cassak, and M. Swisdak, *Geophys. Res. Lett.* **43**, 4145, <https://doi.org/10.1002/2016GL069034> (2016).
- ³⁴H. Karimabadi, D. Krauss-Varban, and N. Omid, *J. Geophys. Res.* **104**, 12,313, <https://doi.org/10.1029/1999JA900089> (1999).
- ³⁵P. L. Pritchett, "Collisionless magnetic reconnection in an asymmetric current sheet," *J. Geophys. Res.* **113**, A06210, <https://doi.org/10.1029/2007JA012930> (2008).
- ³⁶K. Malakit, M. A. Shay, P. A. Cassak, and C. Bard, *J. Geophys. Res.* **115**, A10223, <https://doi.org/10.1029/2010JA015452> (2010).
- ³⁷S. Lu, V. Angelopoulos, and H. S. Fu, *J. Geophys. Res.* **121**, 9483, <https://doi.org/10.1002/2016JA022815> (2016).
- ³⁸X. L. Gao, Y. G. Ke, Q. M. Lu, L. J. Chen, and S. Wang, *Geophys. Res. Lett.* **44**, 618, <https://doi.org/10.1002/2016GL072251> (2017).
- ³⁹J. Egedal, A. Le, W. Daughton, B. Wetheron, P. A. Cassak, L. J. Chen, B. Lavraud, R. B. Torbert, J. Dorelli, D. J. Gershman, and L. A. Avano, *Phys. Rev. Lett.* **117**, 185101 (2016).